Investigation of Capillary Forces Using Atomic Force Microscopy

David L. Malotky and Manoj K. Chaudhury*

Department of Chemical Engineering and Polymer Interface Center, Lehigh University, Bethlehem, Pennsylvania 18015

An atomic force microscope tip, coated with a small amount of liquid silicone, was used to investigate the wetting and capillary bridging forces on various low- and high-energy surfaces. The low-energy surfaces were prepared by reacting alkyl and perfluoroalkyl functional silanes with a silicon wafer (Si/SiO_2). Force–distance scans in air revealed that the silicone fluid forms ductile capillary bridges on the low-energy methyl and perfluoromethyl surfaces, whereas a tight bridge is formed on silica. Further studies on a silicon wafer possessing a gradient of surface energy shed more light on the relationship between surface wettability and capillary forces. These observations can be modeled in a general way using the Young–Laplace equation. The understanding of these capillary interactions at nanoscopic levels may have important applications, especially in the controlled deposition of liquid droplets on surfaces.

Introduction

Atomic force microscopy (AFM) has widely been used to investigate the surfaces of solids in a variety of ways, which include examination of surface topography[1] and investigations of adhesive interactions[2,3] at the sub-microscopic level. By comparison, investigations of liquid surfaces by AFM have been rather limited, even though the liquid capillary forces are among the dominant interactions that prevail in many AFM measurements.

The first systematic study of liquid surfaces by AFM was carried out by Mate et al.,[4] who investigated the properties of a lubricating film of perfluoroether deposited on a silicon wafer. These studies revealed several useful capabilities of AFM. First of all, the measurements yielded local estimates of liquid film thickness that were not possible with conventional optical techniques.[4,5] Second, estimates of disjoining pressure within a thin film, as well as the Laplace pressure within the capillary bridge at the tip–substrate junction, could also be obtained from such measurements. Investigations of these thin film properties are of considerable value, not only from the fundamental understanding of thin film phenomena, but in the rapidly growing arenas of nanotechnology as well.

A recent example of such a nanotechnology is dip pen nanolithography,[6] in which the capillary bridging between an AFM tip and a substrate needs to be controlled. By expanding upon this basic idea of transferring material present on the AFM tip to a substrate, nanoscale surface features may also be produced. Liquid drops of desired volume could be deposited on a surface to produce solid spherical caps for BGA (ball grid array)-type technology,[7] or as nanoglues to attach microscopic objects to a substrate. Although the possibilities of such types of applications are vast, their successful implementations depend on a better understanding of the capillary and thin film phenomena at the submicroscopic level.

The main objective of this study is to examine the capillary bridging behavior of liquids using AFM and to understand how it is controlled by the surface energy of the substrate. By expanding upon this theme, we also investigate to what extent these studies could be used to describe phenomena occurring at nanoscopic junctions. We wish to point out that measurement and modeling of capillary forces, by themselves, do not pose much of a challenge as several such studies have been carried out recently.[8,9] However, carrying out such studies with a conventional AFM tip is complicated by the unknown and irregular geometry of the tip. From the viewpoint of fundamental understanding of capillary forces, it would be desirable to conduct model studies by attaching a bead of known geometry to the AFM tip.[10] However, current technologies allow attachment of beads that are too large for investigating phenomena at a submicron level. A conventional AFM tip, despite its limitations, provides a good option for these types of studies. However, to interpret the observations as accurately as possible, we have carried out these studies with substrates of various surface energies, including a surface possessing a gradual variation in wettability. From such studies, a composite picture of the capillary bridging phenomena at nanoscopic junctions has been developed, which provides insights into the parameters that are responsible for the controlled deposition of liquids on surfaces via AFM.

Results and Discussions

Preparation of the AFM Tip. To accomplish the above objectives, our first task was to transfer a small amount of a model liquid to the tip of an AFM probe. We used a vinyl-functional poly(dimethylsiloxane) (PDMS, MW = 3700) as a model liquid because of its low surface tension and negligible vapor pressure at room temperature. An

* To whom correspondence should be addressed.

(1) Binnig, G.; Quate, C. F.; et al. *Surf. Sci.* **1987**, *1*, 189.

(2) Weisenhorn, A. L.; Hansma, P. K.; Albrecht, T. R.; Quate, C. F. *Appl. Phys. Lett.* **1988**, *54*, 2651.

(3) Burnham, N. A.; Colton, R. J.; Pollock, H. M. *Nanotechnology* **1993**, *4*, 64.

(4) Mate, C. M. *Phys. Rev. Lett.* **1992**, *68*, 3323. Mate, C. M.; Lorenz, M. R.; Novotny, V. J. *J. Chem. Phys.* **1989**, *90*, 7550.

(5) Doppenschmidt, A.; Butt, H. J. *Langmuir* **2000**, *16*, 6709.

(6) Piner, R. D.; Zhu, J.; Hong, S.; Mirkin, C. A. *Science* **1999**, *238*, 661.

(7) Hwang, J. S. *Ball Grid Array and Fine Pitch Interconnections*; Electrochemical Publications: Bristol, 1995.

(8) Pitois, O.; Moucheront, P.; Chateau, X. *J. Colloid Interface Sci.* **2000**, *231*, 26.

(9) Simons, S. J. R.; Fairbrother, R. J. *Powder Technol.* **2000**, *110*, 44.

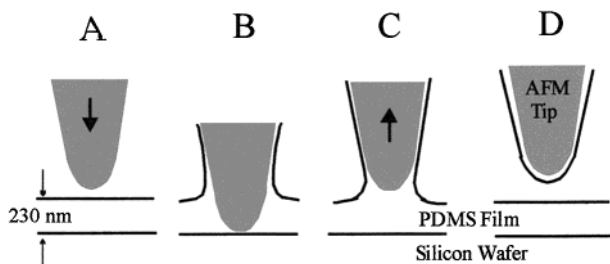(10) Ducker, W. A.; Senden, T. J.; Pashley, R. M. *Nature* **1991**, *353*, 239.

Figure 1. Schematic of the method used to transfer PDMS liquid to the tip of an AFM probe. In our experiments, an unmodified silica tip (A) is dipped into a thin (~230 nm) film (B) of PDMS (MW = 3700) supported on a silicon wafer. The liquid polymer wicks up the probe tip, and upon removal (C), a small amount of fluid is transferred to the tip (D). This liquid-coated tip was then used in force–distance scans on various solid surfaces.

additional advantage of this liquid is that it can be cross-linked by means of the well-known hydrosilation reaction, thus making it amenable to AFM imaging after it is transferred onto a given surface.

A small amount of liquid poly(dimethylsiloxane) of MW = 3700 was transferred onto an AFM probe by scanning the tip vertically against a thin (~230 nm) film of the polymer spin-cast on a silicon wafer. As the tip is retracted from the thin film, a small amount of PDMS is transferred to the probe (Figure 1), which could then be used as a model droplet for the wetting and capillary bridging studies. This liquid transferred to the tip, however, has a very high curvature near the tip apex. Thus, the resultant Laplace pressure induces the liquid to flow away from the tip apex toward its sides. The net thickness of the fluid at the tip apex is thus very small, on the order of 7 nm, as found from subsequent experiments, while the bulk of the liquid accumulates on the sides of the tip.

Capillary Bridging and Surface Wettability. The PDMS-coated AFM tip was used to study the capillary interactions on a variety of substrates having a broad range of surface energies. These substrates include native silicon dioxide on a silicon wafer (Si/SiO$_2$), and the self-assembled monolayers of alkyl (O$_{3/2}$Si(CH$_2$)$_{15}$CH$_3$) and perfluoroalkyl (O$_{3/2}$Si(CH$_2$)$_2$(CF$_2$)$_7$CF$_3$) siloxanes supported on a silicon wafer. The advancing and receding contact angles of PDMS are ~10° and 5° on the hydrocarbon surface and 59° and 46° on the fluorocarbon surface, respectively. Both the advancing and receding angles are 0° for the silica surface. On the basis of these contact angle parameters, unlimited wetting of PDMS is expected on silica, whereas limited spreading is expected on hydrocarbon and fluorocarbon surfaces.

As an unmodified AFM tip approaches a substrate, it experiences negligible attraction until it is very close to the substrate. The van der Waals and/or other short range forces cause the tip to jump into contact with the substrate as soon as the force gradient acting upon the tip exceeds the cantilever spring constant. This kind of cantilever instability is ubiquitous in AFM studies and typically occurs at distances of ~2 nm of tip–substrate separation. However, when a PDMS-coated AFM tip is advanced toward the hydrocarbon and fluorocarbon functionalized surfaces, the instability occurs at ~7 nm of tip–substrate separation. This larger instability distance is indicative of a very thin PDMS liquid film present at the end of the AFM tip.

When the liquid-coated AFM tip is completely separated from and re-advanced toward the substrate, the observed jump in distance typically increases from that (7 nm) of the first contact. On the hydrocarbon (Figure 2) and
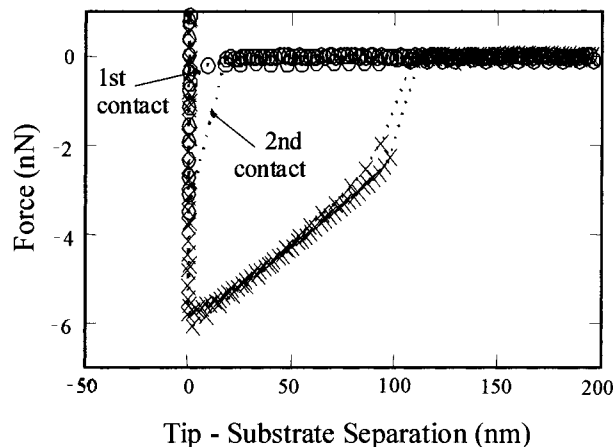

Figure 2. An AFM tip approaches (○) toward and retracts (×) from a hydrocarbon functionalized surface. The jump in distance changes from the first to second scan. During the first scan, the jump to rigid contact with the substrate is indicative of only a thin polymer layer present on the tip. Upon later contacts, however, liquid bridge formation and rupture deposit a droplet of polymer on the surface that increases the jump in distance. The size and shape of the retraction traces remain relatively constant. For these scans, the time between first and second contact was ~3 s.
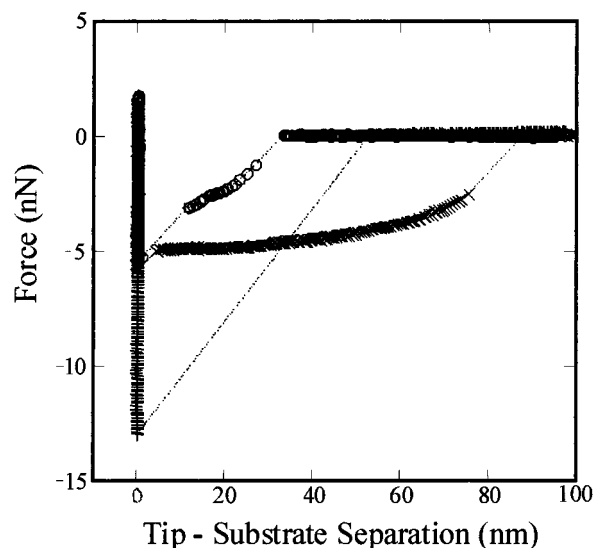

Figure 3. The retraction trace of force–distance scans taken with a 3700 MW PDMS-coated tip on three types of surfaces: hydrocarbon (×), fluorocarbon (○), and silica (+). These scans were taken during the second contact of the tip with the substrate. Extensive capillary bridging is seen on the hydrocarbon and fluorocarbon substrates. By comparison, the capillary bridge is not observed on the silica surface. The contact angles of the 3700 MW PDMS on these surfaces are as follows: hydrocarbon $\theta_a = 10°$, $\theta_r \sim 5°$, fluorocarbon $\theta_a = 59°$, $\theta_r = 46°$, and silica 0°.

fluorocarbon surfaces, these new distances are about 18 and 13 nm respectively, which remain unchanged during subsequent contacts. The larger jump-in distance during the second and subsequent contacts occurs due to the coalescence of the liquid on the AFM probe and the small amount of liquid left behind at the substrate during the rupture of the capillary bridge in the preceding scan. When such a coalescence occurs, capillary forces act on the tip pulling it toward the substrate from a distance much larger than that observed with van der Waals forces.

During the retraction of the probe, various force–distance responses are observed depending upon the surface energy of the substrate (Figure 3). Typically,
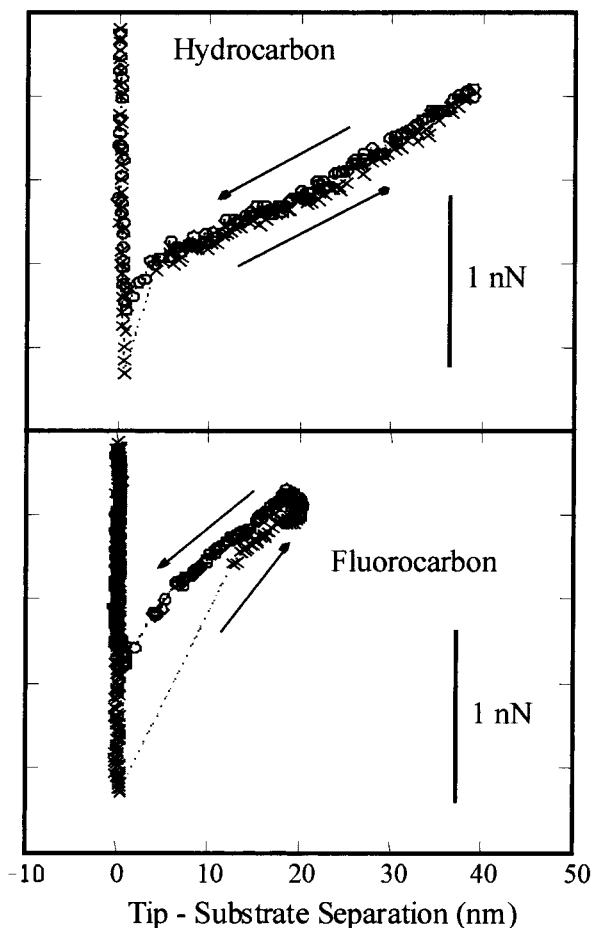
Figure 4. The bridging liquid meniscus is extended without rupture on the hydrocarbon and the fluorocarbon surfaces (○ approach, × retract). The force−distance values exhibit only a small hysteresis far away from the surfaces, indicating that these capillary bridges are in mechanical equilibrium with the liquid on the tip. Large hysteresis is observed when the tip is very close to the substrates.

ductile capillary bridges are formed on the hydrocarbon and fluorocarbon surfaces, whereas a highly nonductile bridge is formed on the silica surface.

Because of the ductile nature of the liquid bridges on the hydrocarbon and fluorocarbon surfaces, it is possible to advance and subsequently retract the AFM probes through the liquid bridges without rupturing them (Figure 4). These measurements exhibit only little hysteresis of the capillary force when the tip−substrate separation is greater than 3 nm on the hydrocarbon surface and greater than 7 nm on the fluorocarbon surface. These negligible hystereses indicate that the liquid in the capillary junction is nearly in mechanical equilibrium with the liquid reservoir on the tip itself. Viscous forces are estimated[8] to be approximately 2×10^{-15} N, far less than can be measured with our AFM, where the noise level is on the order of 10^{-11} N. The finite hystereses observed on both the hydrocarbon and fluorocarbon surfaces at distances less than 3 and 7 nm, respectively, suggest that some sort of nonequilibrium process may be operating while the tip is very close to the substrate.

Similar experiments could not be performed on bare silica (Si/SiO₂). Here, once the initial tip−substrate contact is ruptured, the surface tension force acting through the liquid meniscus is not large enough to counteract the restoring force of the cantilever, when the tip jumps out of contact. The limited liquid meniscus present between the tip and the silica substrate may, however, be the cause
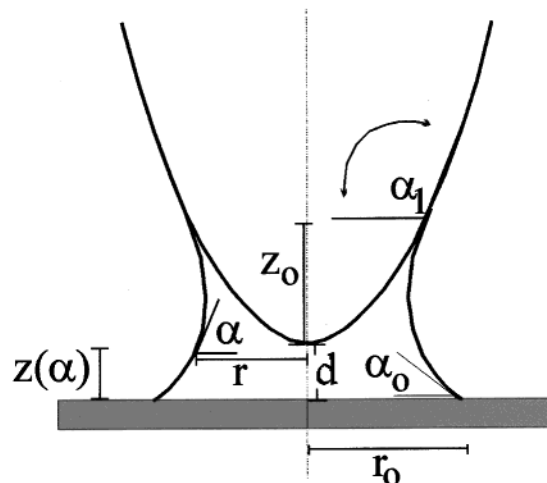

Figure 5. Schematic of a liquid bridge between an AFM tip and a flat surface.

for the large adhesive force observed on this surface, as discussed later.

   Theory of Capillary Force. According to the theory of capillarity, the force acting on the AFM tip has two components. The first is the Laplace force arising from the difference between the pressures acting on the inside and outside of the liquid bridge, and the second is the surface tension force acting along the free surface of the liquid.[11] In general, the mean curvature of the free liquid surface can be described by the following differential equation:

$$2H = \frac{\mathrm{d}^2 z/\mathrm{d}r^2}{(1 + (\mathrm{d}z/\mathrm{d}r)^2)^{3/2}} + \frac{\mathrm{d}z/\mathrm{d}r}{r(1 + (\mathrm{d}z/\mathrm{d}r)^2)^{1/2}} \quad (1)$$

Here z and r define the coordinate of the free surface. The Laplace pressure difference is proportional to the mean curvature of the free surface, and its magnitude would be zero (i.e., $H = 0$) when a mechanical equilibrium is achieved between the liquid present in the bridge and that on the tip.

   Negligible hystereses in the force−distance scans of the previous section (Figure 4) indicate that this mechanical equilibrium is likely achieved. Hence, we treat the mean curvature H in eq 1 as equal to zero so that the force acting on the tip results from surface tension alone. By setting $H = 0$, eq 1 can be integrated to obtain the following results:

$$r \sin(\alpha) = r_0 \sin(\alpha_0) \quad (2)$$

$$z(\alpha) = r_0 \sin(\alpha_0) \ln\left(\frac{\tan(\alpha/2)}{\tan(\alpha_0/2)}\right) \quad (3)$$

where r_0, α, and α_0 are as shown in Figure 5. The surface tension force acting on the tip is given by

$$F = 2\pi r \gamma \sin(\alpha) = 2\pi r_0 \gamma \sin(\alpha_0) \quad (4)$$

Thus the replacement of the term $r_0 \sin(\alpha_0)$ into eq 3 yields the following equation:

$$z(\alpha) = \frac{F}{2\pi\gamma} \ln\left(\frac{\tan(\alpha/2)}{\tan(\alpha_0/2)}\right) \quad (5)$$

   (11) Orr, F. M.; Scriven, L. E.; Rivas, A. P. *J. Fluid Mech.* **1975**, *67*, 723.

Whether or not the mean curvature attains a negative value depends on the detailed geometry of the tip. However, when the zero mean curvature condition prevails, eq 5 predicts an inverse relationship between capillary extension and the contact angle of the liquid on the solid substrate, α_o. To illustrate the above point, let us rewrite eq 5 in the following form:

$$d + z_o = \frac{F}{2\pi\gamma} \ln\left(\frac{\tan(\alpha/2)}{\tan(\alpha_o/2)}\right) \quad (6)$$

The definitions of d and z_o are given in Figure 5. Had the detailed geometry of the AFM tip been known, it would be straightforward to analyze the force—extension data of Figure 3 in the light of eq 6. In the absence of such detailed information, it is still possible to analyze the data of Figure 3 to some extent by realizing that at the same value of F, the set of z_o and α values would be identical on two different surfaces. Thus, if d_1 and d_2 are the tip to substrate separations on fluorocarbon and hydrocarbon surfaces with corresponding values of α_o as α_{1o} and α_{2o} respectively, one can write

$$d_1 - d_2 = \frac{F}{2\pi\gamma} \ln\left(\frac{\tan(\alpha_{2o}/2)}{\tan(\alpha_{1o}/2)}\right) \quad (7)$$

By using eq 7 and the advancing contact angles of PDMS (59° for fluorocarbon and 10° for hydrocarbon), the difference of the capillary extension distances ($d_1 - d_2$) at a bridging force of 2.5 nN is estimated to be ~37 nm. However, using the receding contact angles (46° for fluorocarbon and ~5° for hydrocarbon), the $d_1 - d_2$ value is estimated to be ~45 nm, which is much closer to the experimental value of 57 nm. We note that the values of the contact angles (especially the receding angles) on the hydrocarbon surface are somewhat uncertain because it is rather difficult to measure angles below 15° using a standard goniometer. A receding angle of 3°, instead of 5°, on the hydrocarbon surface would predict a value (56 nm) of $d_1 - d_2$, which agrees exactly with the experimental value. To examine further the relationship between capillary extension and the surface wettability, we have used a substrate possessing a gradual variation of wettability,[12–14] which allows multiple experiments to be performed on a single substrate.

Capillary Bridging on a Gradient Energy Surface. A silicon wafer possessing a gradual variation of wettability was prepared by diffusion-controlled silanization[13,14] of a fluoroalkyl silane. The advancing contact angle of PDMS on this surface was about 45° at one end, and it gradually decreased to zero near the other end (Figure 6). The force—distance data obtained with a PDMS-coated AFM tip on such a gradient surface clearly shows that the capillary extension for a given force increases systematically with surface wettability (Figure 7).

We next examine how these force—distance profiles conform with the Young—Laplace equation by arranging eq 6 in the following form:

$$-\left(\frac{F}{2\pi\gamma}\right) \ln(\tan(\alpha_o/2)) = d + \left\{\frac{-F}{2\pi\gamma} \ln(\tan(\alpha_1/2)) + z_o\right\} \quad (8)$$

Plots of $-(F/2\pi\gamma) \ln(\tan(\alpha_o/2))$ versus d can be constructed

(12) A surface possessing a gradient of surface energy was used by Carter (Carter, S. B. *Nature* **1967**, *213*, 256) to study haptotactic movements of cells, Elwing et al. (Elwing, H.; Welin, S.; Askendal, A.; Nilsson, U.; Lundstrom, I. *J. Colloid Interface Sci.* **1987**, *119*, 203) to study protein adsorption, and Chaudhury et al. to study the migration of liquid droplets.[13,14]
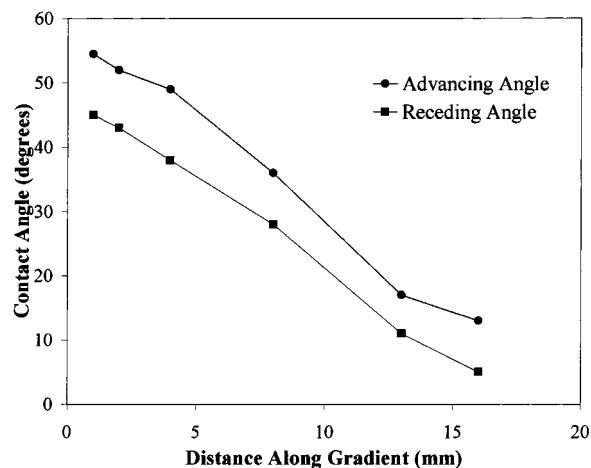

Figure 6. Advancing and receding contact angles as a function of location on a gradient surface, which was prepared by the diffusion controlled silanization of a perfluoroalkyl silane.
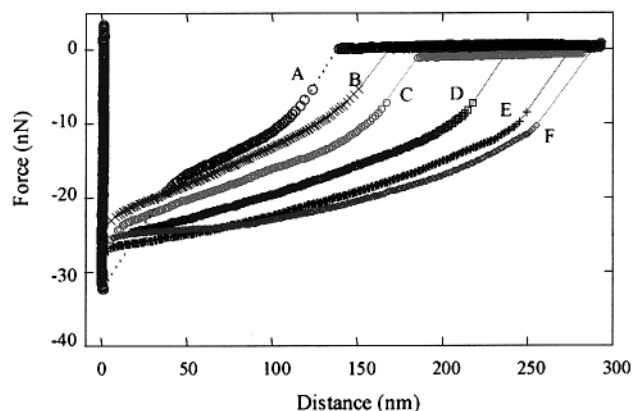

Figure 7. Retraction force—distance traces taken by a PDMS-coated AFM tip on a gradient surface. A retraction scan on the fluorocarbon surface (A) is included as a reference. The other scans were taken at a distance of 1 mm (B), 6.5 mm (C), 12 mm (D), 14 mm (E), and 16 mm (F) from the edge of the wafer. The AFM tip used for these measurements was nearly 5 times larger than that used to aquire the data in Figures 2—4; consequently, the capillary forces are also much larger here.

from Figure 7 using eq 8 by selecting capillary extension data at identical force values on different parts of the gradient. Such a plot should yield a straight line of slope equal to 1, with an intercept that depends on α_1 and z_o, both of which remain invariant for a given value of F.

Figures 8 and 9 show such plots corresponding to force values ranging from 10 to 20 nN on different parts of the gradient zone characterized by a pair of advancing (Figure 8) and receding (Figure 9) contact angles (α_o). Although these plots are linear, their slopes differ from the expected value of unity. A reason for this discrepancy could be that the AFM tip does not have a uniform cross section except very close to its apex. For a tip of noncircular cross section, eq 8 is an overgeneralization. One may argue that for an irregular tip, the assumption of zero mean curvature (and hence zero Laplace pressure) could also be violated; that is, the system is not at equilibrium. However, as discussed in Figure 4, the AFM measurements exhibit negligible hysteresis in the advancement/retraction scans. This indicates that either the condition of zero Laplace pressure is achieved or the liquid does not have enough time to flow

(13) Chaudhury, M. K.; Whitesides, G. M. *Science* **1992**, *256*, 1539.
(14) Daniels, S.; Chaudhury, M. K.; Chen, J. C. *Science* **2001**, *291*, 633.
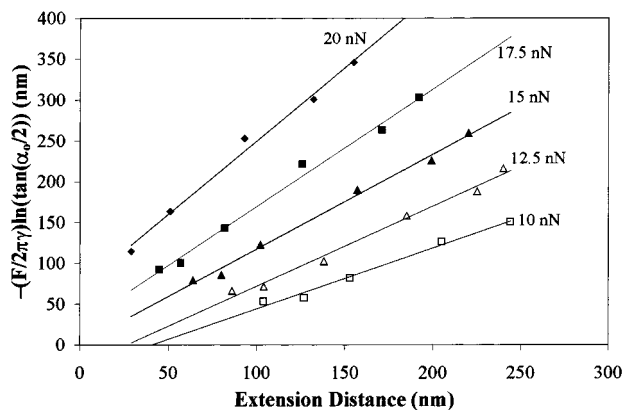
Figure 8. Data from the gradient surface (Figure 6) plotted as a function of advancing contact angle at different force values. The contact angles on different locations of the gradient surface as indicated by A−F on Figure 7 were obtained by interpolations of the contact angle vs distance data shown in Figure 6. The slopes of these lines are as follows: 1.79 ($F = 20$ nN), 1.44 ($F = 17.5$ nN), 1.16 ($F = 15$ nN), 0.98 ($F = 12.5$ nN), 0.75 ($F = 10$ nN).
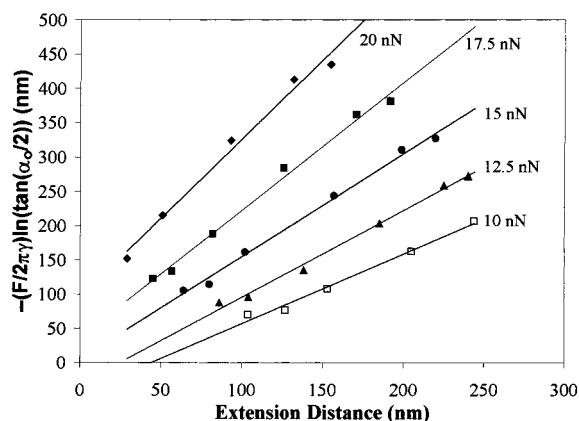

Figure 9. Data from the gradient surface (Figure 6) plotted as a function of receding contact angle at different forces. The slopes of these lines are as follows: 2.30 ($F = 20$ nN), 1.86 ($F = 17.5$ nN), 1.49 ($F = 15$ nN), 1.27 ($F = 12.5$ nN), 1.02 ($F = 10$ nN).

in and out of the drop during the duration of an AFM scan. On the basis of on an order of magnitude estimate, the distance traveled by the liquid PDMS of kinematic viscosity (ν) 0.48 cm²/s within the time of an AFM scan (~3 s) is ($L \sim (\nu t)^{1/2}$) about 1 cm. The typical size of the drops under the AFM is much smaller than the above estimate, thus indicating that viscous forces provide no hindrance to achieving hydrostatic equilibrium within the time frame of the AFM measurements.

There is, however, another scenario to be considered. The slopes of the lines in Figure 8, which are produced using the advancing contact angles, are closer to unity at the high force values than those corresponding to the receding contact angles (Figure 9). When the receding contact angles are used, the slopes of the lines approach the expected value of unity when the force reaches a value of 10 nN, which is just before the rupture of the liquid bridge. A plausible scenario is as follows. When the liquid-coated AFM tip contacts a substrate, the liquid spreading is governed by the advancing contact angle. When the tip is retracted, the contact angle at first changes from the advancing to the receding mode without the movement of the contact line. The set of data corresponding to the higher F values falls in this range. However, as the transition from the advancing to the receding mode occurs at different

values on the gradient surface, the force−distance data are not well behaved when analyzed using eq 8. Only after the tip is sufficiently retracted from the surface (at low liquid bridging force) do the contact angles reach their true receding values on various parts of the gradient surface and, therefore, yield the expected slope of unity when plotted according to eq 8.

When a tip is very close to the substrate, a small hysteresis on the hydrocarbon and a substantial hysteresis on the fluorocarbon surface are observed (Figure 4). This hysteresis is indicative of nonequilibrium behavior of the capillary junction. It could arise if the geometry of the tip and the substrate makes it impossible for the mean curvature of the liquid junction to reach a zero value or if additional adhesive interactions operate between the tip and substrate at such distances. Although this capillary hysteresis is one of the most interesting features of these studies, we have not been able to identify its exact origin at present.

Capillary Bridge on Silica. The force−distance behavior of PDMS on silica (Si/SiO$_2$) is very different from the cases observed with the fluorocarbon and hydrocarbon surfaces. Here, the tip undergoes an instability jump from contact once a critical force is reached. Clearly, no stable capillary bridge is formed on silica; that is, the liquid from the AFM tip is spontaneously drained onto the substrate. Since the contact angle of PDMS on silica is zero, the enormous viscous stress essentially pins the liquid/solid contact line.[15] However, even though the liquid cannot spread by viscous motion, a rough calculation shows that the molecules can still spread at an appreciable rate on the surface by diffusion. For example, the distance traveled by a PDMS molecule on silica is about $1-3$ μm within the time (~1 s) that the AFM tip is in contact with the substrate.[16] The volume of PDMS transferred by surface diffusion[17] during this time period is about $(2.2-30) \times 10^6$ nm³, which is at least comparable to the volume of the liquid bridge on the hydrocarbon surface just before rupture (2.3×10^6 nm³). Thus, because of the huge drainage of PDMS by surface diffusion, it cannot accumulate to form a stable liquid bridge on the silica surface. The complete wettability (i.e., zero contact angle) of PDMS on silica results in a negative mean curvature of the meniscus, holding the tip tightly in contact with the substrate by the dominant Laplace force. Once the initial contact is broken, there is not enough surface tension force acting within this meniscus to offset the restoring force on the cantilever, and the tip jumps out of contact with the silica substrate.

The forces between the AFM tip and silica surface cannot be modeled in the same way as it is done on the fluorocarbon and the hydrocarbon surfaces due to the nonequilibrium drainage of liquid. Here the negative Laplace pressure within the liquid bridge is somewhat governed by the disjoining pressure (Π) within the PDMS film that spreads ahead of the liquid as a precursor film.[4] This disjoining pressure can be estimated using the following equation:

$$\Pi = \frac{A}{6\pi\delta^3} \tag{9}$$

where A is the Hamaker constant, and δ is the thickness of the precursor film. By considering a typical value of A

(15) De Gennes, P. G. *Rev. Mod. Phys.* **1985**, *57* (3, Pt. 1), 827 and references therein.

(16) From the observations of Silberzan and Leger (Silberzan, P.; Leger, L. *Macromolecules* **1992**, *25*, 1267), the diffusion constant (*D*) for 3700 MW PDMS is estimated to be in the range $10^{-11}-10^{-12}$ m²/s. The distance the PDMS molecule could diffuse is ~$(Dt)^{1/2}$ in time *t*.

as 4.0×10^{-20} J and δ as the thickness (0.7–1 nm) of the PDMS molecules, the disjoining pressure within the precursor film is estimated to be about 8×10^6 N/m². As this disjoining pressure is roughly similar to the Laplace pressure within the capillary bridge,[19] the radius of curvature of the meniscus of the liquid bridge is estimated to be only about 2.5 nm. This is much smaller than the radius ($\sim$50 nm) of the AFM tip. Since this meniscus is very thin, the force needed to detach the AFM tip from the silicon wafer can be estimated using the following equation:[11]

$$F = 4\pi R\gamma \qquad (10)$$

Here R is the radius of curvature of the AFM probe very close to its tip, which was estimated to be about 50 nm from its image taken with the TGT-01 calibration grating[20] (NT-MDT). Using the value of R as 50 nm and the value of γ as 20 mN/m, eq 10 predicts a pull-off force of 12 nN, which is close to that (13 nN) measured experimentally.[21]

Deposition of Nanodrops. The general understanding of the capillary interaction between the liquid-coated AFM tip and a substrate gained from the above studies can be used to control the deposition of nanoscopic drops on a surface. Deposition of these nanodrops requires a liquid bridge between the tip and the substrate that could be extended and ruptured, thus leaving behind a significant volume of material on the substrate. These conditions are satisfied, as evident in Figure 3, for the liquid bridging on the fluorocarbon and hydrocarbon surfaces. Of these two, a given tip leaves behind a thicker droplet of liquid on the hydrocarbon surface, and therefore this surface was used initially to ensure that enough polymer is transferred to the substrate. To achieve this objective, we used the vinyl endcapped dimethylsiloxane (MW = 3700) that carried a small amount of methylhydrogensiloxane cross-linker and a platinum catalyst. This allowed for a hydrosilation reaction between the SiH groups of the cross-linker and the vinyl groups of the polymer resulting in a cross-linked network of PDMS after it was transferred to the substrate.

When deposition and cross-linking of the PDMS elastomer were attempted using a tip of radius $\sim$50 nm, spherical caps were not observed in the regular pattern as deposited. Only a small number of droplets of the expected size (spherical caps 10 nm thick and 114 nm in radius) were seen on the surface in images taken after cross-linking. For these small tips, although significant liquid bridging was observed in the force–distance scans, cross-linking by hydrosilation did not appear to proceed

(17) A crude estimate of this volume (v) is given by $v = \pi eDt$, where e is the thickness of the molecular film, D is the diffusion coefficient, and t is the time (1.0 s). A conservative (lower) estimate of e is the thickness of the molecular film, that is, 7–10 Å, as observed by Cazabat et al.[18] and Leger et al.[16]

(18) Voue, M.; Valignat, M. P.; Oshanin, G.; Cazabat, A. M.; De Conick, J. *Langmuir* **1998**, *14*, 5951. Cazabat, A. M.; Valignat, M. P.; Villette, S.; De Coninck, J.; Louche, F. *Langmuir* **1997**, *13*, 4754 and references therein.

(19) The disjoining pressure is not strictly equal to the Laplace pressure as the liquid continues to flow because of the gradient of disjoining pressure.

(20) This grating consists of an array of tips with a small radii of curvature (<10 nm) and tip angle (<20°). Imaging of this grating in contact mode produces a convolution of the grating tip and the experimental tip. This technique is useful for determining the approximate dimensions of an experimental tip.

(21) While this agreement is quite excellent, we wish to point out that a similar experiment performed on a silicon wafer just after it is treated with an oxygen plasma yields a force as high as 20 nN. A force of this magnitude cannot be explained on the basis of the Laplace equation alone. We believe that the origin of such high adhesive forces could be the bridging interactions between the tip and substrate caused by the PDMS chains.
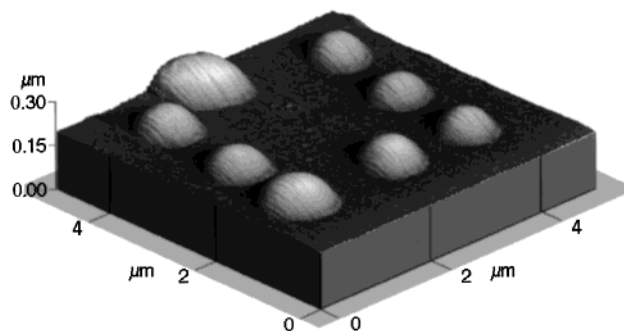

Figure 10. Hemispherical caps of PDMS elastomer produced on a hydrocarbon surface by an AFM tip. These caps were deposited by performing force–distance scans on the surface in a grid with 1.6 μm spacing. Examination of the figure reveals that the central drop has coalesced with an outer drop. Also, this drop appears out of place in comparison with the others, perhaps because of a motion induced by a thermal or chemical Marangoni effect, which could have been induced either by inhomogeneous heating during the cure cycle or by a defect on the surface.

smoothly. A larger tip of radius $\sim$150 nm, however, yielded the desired result.

Using the 150 nm radius tip, a significant amount of liquid transfer was possible on the hydrocarbon surface. These droplets could be easily cross-linked into elastomeric caps by heating them to about 120 °C for 40 min. The elastomeric caps could be subsequently imaged with a different AFM tip. A surface decorated with nanodrops is shown in Figure 10. The contact angles of these droplets on the hydrocarbon surface as estimated from the line scans of the drops[22] range from 7 to 10°, which compares favorably with that (9.5°) of a macroscopic drop of the PDMS fluid on the hydrocarbon surface.

Concluding Remarks

Atomic force microscopy can be used to study the relationship between capillary bridging interactions and the surface wettability. Experiments with low-energy surfaces and with a surface possessing a gradient of surface energy show that the extension of the capillary bridge increases with the substrate wettability. As long as the contact angle remains nonzero, the capillary bridge exhibits an equilibrium shape, which is dictated by the contact angle at the solid–liquid interface. The capillary extension before the rupture of the liquid bridge varied systematically with the local solid–liquid contact angle. However, when the contact angle becomes zero, the liquid bridge exhibits a nonequilibrium behavior, where fast spreading of the precursor film appears to drain the liquid from the tip–substrate junction. While surface tension acting on the meniscus is the dominant force on the tip for finite liquid–solid contact angles, the tip is held tightly on the completely wettable surface by the dominant Laplace force. These studies assist us in precise deposition of liquids on surface by the manipulation of capillary forces. Small amounts of liquid thus transferred can be cross-linked to form elastomeric caps. It is hoped that these liquid and elastomeric caps could be useful as nanoglues or in surface mount technologies.

Experimental Section

General Information. All force–distance measurements were performed with a Park Scientific Autoprobe CP atomic force microscope. The spring constants[23] of the AFM cantilevers ranged from 0.2 to 0.4 N/m. The approximate apex radius of each tip

(22) Vitt, E.; Shull, K. R. *Macromolecules* **1995**, *28*, 6349.

used in the investigation was found by performing a topography scan with that tip on a TGT-01 calibration grating[18] (NT-MDT). Force−distance scans of the type shown in Figure 3 were taken in air both at ambient humidity (30−50%) and under nitrogen (<12% humidity). There was no observable quantitative or qualitative difference between the scans taken in these two environments suggesting that the capillary condensation of water was not an issue for our system. The tip speed used for all experiments was 0.3 μm/s, and the tip remained in contact with the substrate for approximately 1 s during each scan. All the advancing and receding contact angles of silicone liquid were measured with a Rame' Hart goniometer. Drops were deposited and withdrawn from the surfaces using a Gilmont microsyringe.

The model liquid in this study was vinyl-endcapped dimethyl siloxane oligomer (poly(dimethylsiloxane), PDMS) of molecular weight 3700 with a polydispersity index of ∼1.5 and a viscosity of 0.48 poise. The polymer was transferred to the AFM tip by scanning it repeatedly into a thin (230 nm) film of the liquid spin-coated on a silicon wafer.[1] A significant quantity of liquid needs to be transferred to the tip to form a semi-infinite liquid reservoir at the tip surface. To this end, the tip was typically dipped into the liquid film at least six times to ensure enough liquid had been transferred.

The above silicone fluid was slightly modified when it was used to form the nanoscopic surface features. This liquid consisted of the same vinyl-endgrouped dimethyl siloxane oligomer (3700 MW, $D_p = 50$), to which was added 6 wt % of methyl hydrogen siloxane cross-linker and 2 wt % of a silicone fluid containing platinum catalyst to carry out the hydrosilation reaction. All these components were obtained from Dow Corning Corp. For reasons that were discussed above, a blunt AFM tip ($R \approx 150$ nm) with a spring constant of 0.45 N/m was used to deposit this liquid to be cured into spherical caps. The liquid mixture was transferred to the AFM tip by scanning it in a thin film of the liquid supported on a silicon wafer. The coated tips were used to perform force−distance scans in a grid (1.6 μm between points) on a silanized (CH$_3$(CH$_2$)$_{15}$SiCl$_3$) silicon wafer. The deposited

drops were cross-linked at 120 °C for 40 min, after which the resulting surface was imaged in overdamped AC (noncontact) mode.

Model Surfaces. Adsorbed monolayers of alkyl (O$_{3/2}$Si-(CH$_2$)$_{15}$CH$_3$) and perfluoroalkyl (O$_{3/2}$Si(CH$_2$)$_2$(CF$_2$)$_7$CF$_3$) functional siloxane were prepared according to a method described elsewhere.[11] Here only a brief description is given. Small strips of silicon wafer were cleaned by immersing them in hot piranha solution (H$_2$SO$_4$/H$_2$O$_2$ = 7:3 v/v) for 45 min. These strips were subsequently rinsed in distilled−deionized water and blown dry with nitrogen. The strips were then exposed to oxygen plasma for 45 s and immediately reacted with the vapor of either the alkyl (Cl$_3$Si(CH$_2$)$_{15}$CH$_3$) or the perfluoroalkyl (Cl$_3$Si(CH$_2$)$_2$(CF$_2$)$_7$-CF$_3$) functional chlorosilanes in reduced pressure (0.2 Torr). Some of the wafer strips were cleaned by oxygen plasma for AFM investigation. Before each AFM experiment, the silicon wafer was cleaned in oxygen plasma, which yielded a high-energy surface. The other surfaces were cleaned with chloroform before use.

A silicon wafer possessing a gradient of wettability was prepared according to the methods described previously.[13,14] In that, a cotton string soaked with pure perfluorodecyltrichloro-silane (Cl$_3$Si(CH$_2$)$_2$(CF$_2$)$_7$CF$_3$) was used as a source of silane. One end of a cleaned silicone wafer (cleaned sequentially by acetone, ethanol, and flame and then dried and cooled in dry N$_2$) was placed at a distance of 2 mm under the cotton string. As the silane evaporated from the string, it diffused in air while reacting with the silicon wafer. The wettability of the silicon wafer was modified in proportion to the amount of adsorbed silane. The silicon strip was exposed to the diffusing silane for 4 min in a low-humidity (<10%) chamber. Low humidity was necessary to keep adsorbed water from competing with the diffusing silane for surface silanol (−Si−O−H) groups. The typical wettability gradient of the silicon wafer probed by a silicone fluid of MW ≈ 3700 is shown in Figure 6.

(23) Force constants were calculated using the method described in Cleveland, J. P.; Manne, S.; Bocek, D.; Hansma, P. K. *Rev. Sci. Instrum.* **1993**, *64*, 403.